ELSEVIER

Surface and Coatings Technology 74–75 (1995) 1020–1027

SURFACE & COATINGS TECHNOLOGY

Decorative boride coatings based on LaB_6

C. Mitterer [a], J. Komenda-Stallmaier [a], P. Losbichler [a], P. Schmölz [b], H. Störi [b]

[a] *Institut für Metallkunde und Werkstoffprüfung, Montanuniversität, Franz-Josef-Straße 18, A-8700 Leoben, Austria*
[b] *Institut für Allgemeine Physik, Technische Universität, Wiedner Haupstraße 8–10, A-1040 Wien, Austria*

Abstract

Decorative coatings of lanthanum boride were deposited onto steel and molybdenum substrates employing d.c. magnetron sputter deposition using LaB_6 targets. The characterization of the coatings was achieved by means of scanning electron microscopy, electron probe microanalysis and X-ray diffraction. The results were discussed in connection with application-related properties, such as film hardness and colour determined by Vickers microhardness and CIE-$L^*a^*b^*$ colorimeter measurements. The aim of this work was the investigation of the interrelationships between the chemical composition, microstructure, hardness and colour of the coatings. Sputtering of LaB_6 targets results in the formation of extremely fine columnar films with predominantly (100)-oriented LaB_6 crystals. With increasing process gas pressure, an increase in the (100) texture and a decrease in the lattice distortion were observed. Likewise, the boron-to-lanthanum atomic ratio decreased from 6.8 to 6.5. With increasing argon pressure, a distinct decrease in the brilliance value L^* was observed, resulting in a shift in colour from dark violet to almost black. The maximum Vickers microhardness of the coatings was approximately 2900 $HV_{0.01}$. The results of the investigations establish the correlations between the stoichiometry, microstructure, hardness and film coloration for decorative coatings based on LaB_6.

Keywords: Sputtering; Decorative coatings; Lanthanum hexaboride; Microstructure; Properties

1. Introduction

The hexaborides of the rare earth elements are being considered for applications as hard, wear- and corrosion-resistant coatings, particularly, for the decoration and protection of consumer products such as eyeglass frames, wristwatch casings and wristbands or writing implements [1]. Of the many hexaborides available, lanthanum hexaboride (LaB_6) is especially attractive, because of its purple–red colour and its high chemical stability [2–4]. Films based on LaB_6 may provide a welcome opportunity to extend the existing chromatic spectrum of available decorative coating colourations. Currently, the primarily sputter-deposited decorative coatings are usually based on nitrides or carbonitrides of titanium or titanium alloys, with an essentially limited spectrum of colour tones, ranging from golden yellows, through various shades of grey to black [5–7].

LaB_6 has the simple body-centred-cubic (b.c.c.) B2 (CsCl) structure. It is characterized by a three-dimensional skeleton of B_6 octahedra, the interstices of which are filled by lanthanum atoms [8,9]. The crystal structure is dominated by strong B–B bonds. LaB_6 exists over a wide composition range (from LaB_6 to $LaB_{7.8}$ [10]) without significant deviations of the lattice parameter. The deviations from stoichiometry are accomodated by the formation of lanthanum vacancies. LaB_6 exhibits a pronounced spectral reflectivity minimum at a wavelength of about 590 nm, as a result of plasma oscillations [3,11], i.e. resonant interactions between the electromagnetic wave of the incident light and free electrons. McKelvy et al. [12] reported a gradual shift in the coloration with increasing B/La atomic ratio, going from purple–red ($B/La \approx 6$) to blue tones ($B/La > 6.07 \pm 0.03$).

Some fundamental properties of sputter-deposited coatings based on LaB_6 have been reported in an earlier paper [13]. The aim of this study was to investigate the correlation between the chemical composition, structure and coloration of LaB_6 coatings. In addition, their potential for application as decorative coatings should be evaluated by microhardness measurements and corrosion tests.

2. Experimental

Coatings were produced by means of a previously described [14] d.c. magnetron sputtering unit. The substrates used were molybdenum sheets and metallographically polished steel discs (quenched and tempered steel

0257-8972/95/$09.50 © 1995 Elsevier Science S.A. All rights reserved

34 CrNiMo 6 and austenitic steel X5 CrNi 18 10) precleaned with ethylene in an ultrasonic cleaner. The target used was a commercially available LaB_6 disc (diameter, 150 mm). The process gas used was argon with a purity of 99.999%. The target–substrate distance in this configuration was 55 mm. The coating parameters systematically varied during deposition runs included the argon flow rate, the bias voltage and the substrate temperature. The thicknesses of the coatings reached 3 ± 1 μm.

The deposition rates and film thicknesses were determined using a quartz film thickness sensor and monitor (Edwards FTM 3) with the theoretical density of LaB_6 (4.73 g cm^{-3} [15]) and a spherical abrasion method ("Calotest"[16]). The morphology of the films was studied using a Cambridge Instruments Stereoscan 360 scanning electron microscope. The chemical composition of the deposits was determined by electron probe microanalysis (EPMA; Cameca Camebax MB1) [17]. Quantification occurred by means of a bulk LaB_6 standard. The results were cross-checked by nuclear scattering methods (elastic recoil detection (ERD) and Rutherford backscattering (RBS)). The X-ray diffraction (XRD) spectra were recorded with a Siemens F goniometer, using Cr Kα radiation. The film hardness was measured using a Vickers microhardness tester (Reichert-Jung MD 4000) with a load of 9.8 cN (10 p) and an optical microscope (magnification, 1600 ×). The given values are the average of seven different indentations. Colour characterization by CIE-$L^*a^*b^*$ units was carried out using a Dr. Lange Micro Colour LMC colourimeter (light source, D65; measurement geometry, d/8). Corrosion tests were performed by subjecting coated austenitic samples to the saturated vapour from an artificial perspiration solution [18] at a temperature of 40 °C.

3. Results and discussion

Among the systematically varied deposition parameters, the argon flow rate showed the strongest effect on the film structure and properties. Growth rates of about 80–90 nm min^{-1} were achieved in sputtering from the LaB_6 target at a sputtering power density of 2.8 W cm^{-2}. Fig. 1 shows the dependence of the deposition rate on the argon flow, which was varied in the range 70–150 sccm, resulting in pressures between 0.7 and 2.8 Pa. Despite the different deposition parameters used for the quartz film thickness sensor measurements (grounded and water-cooled sensor) and the spherical abrasion method (bias voltage, −100 V; substrate temperature, 200 °C), we observed an excellent agreement between both curves. Taking into account the observed weak effect of the bias voltage and the substrate temperature on the growth rate, we can assume that the actual coating density is very close to the theoretical density used for the quartz film thickness sensor measurements. The decrease in the deposition rates with increasing argon flow rate shown in Fig. 1 can be explained by the increased number of collisions of the sputtered energetic particles with argon atoms, resulting in a larger number of thermalized atoms [19,20] with reduced deposition probabilities.

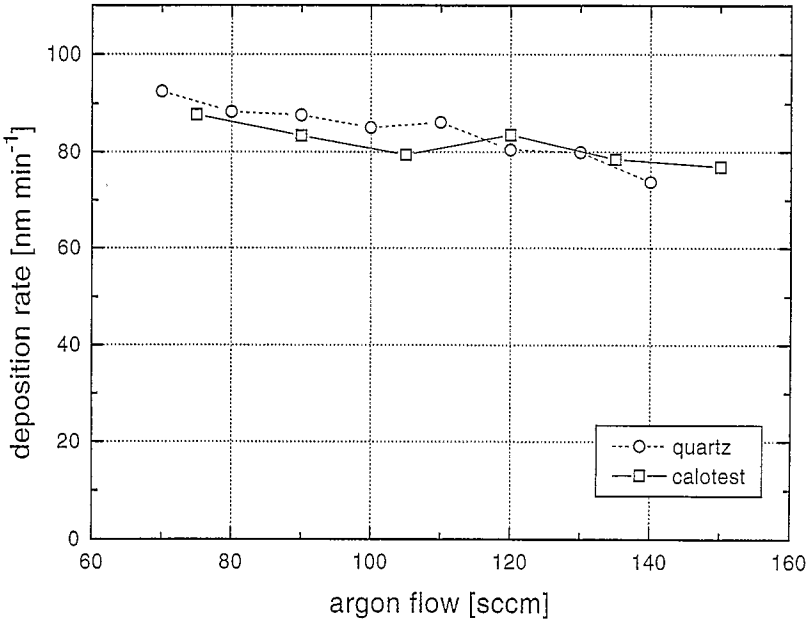

Fig. 1. Deposition rate measured with the quartz film thickness sensor and monitor ("quartz") and that calculated from the final coating thickness using the spherical abrasion method ("Calotest") and the corresponding deposition time as a function of the argon flow rate: quartz — sputtering power, 500 W; grounded and water-cooled sensor; Calotest — sputtering power, 500 W; bias voltage, −100 V; substrate temperature, 200 °C.

Fig. 2 shows a scanning electron microscopy (SEM) fracture cross-section of a coating deposited onto a molybdenum substrate. The dense, extremely fine columnar structure obtained was formed using deposition conditions with a moderate energetic contribution for film growth. In the complementary growth region, i.e. an extremely low or high energetic contribution (especially at high argon flow rates, high bias voltage or low substrate temperature), the structure of the coatings becomes extremely fine grained to fracture amorphous. Obviously, columnar film growth is not possible with the low energies of sputtered target atoms (at high argon flow rates) or high energy ion bombardment (at high bias voltages) [22,23]. Very similar results have been obtained in a transmission electron microscopy (TEM) study on sputtered zirconium boride films [14]. Combinations of these extreme deposition conditions resulted in coatings with low adherence. The very crucial deposition parameter with respect to the adherence was the substrate temperature, with a maximum value for stable coatings of 250 °C.

Films deposited at low argon flow rates or high bias voltages showed a pronounced tendency to form surface defects such as craters or droplets (cf. the surface of the coating cross-section in Fig. 2). This behaviour results from high cathode potentials (at the target, at low argon pressures; at the substrate, at high bias voltages), resulting in an increased possibility for arc ignition [24], especially when using compound targets with low density.

The chemical composition of the coatings is plotted in Fig. 3 as a function of the argon flow rate. All the films deposited were overstoichiometric — the B/La atomic ratio yielded values above 6.2. In non-reactive sputter processes, stoichiometric deviations of the coating from the target composition are attributable to interactions of the sputtered target atoms with the plasma discharge in the transport phase and at the surface of the growing film, assuming that diffusion processes in the target are inhibited [25]. Therefore, special notice should be paid to the difference between the atomic masses of lanthanum (138.9) and boron (10.8). This means that the scattering probabilities of these atoms in the discharge space by argon are very different from each other, although the energy transfer functions ε [26], i.e.

$$\varepsilon = \frac{4m_t m_{Ar}}{(m_t + m_{Ar})^2} \quad (1)$$

where m_t and m_{Ar} are the atomic masses of the target and argon atoms, respectively, are very close together (lanthanum, 0.69; boron, 0.67). In particular, the collision cross-section depends strongly on the particle radius [27] and is very small for boron atoms.

The general overstoichiometry of the deposited coatings may be explained by the high mobility of boron atoms within the discharge, which then arrive comparatively easily at the substrate, especially at low argon pressures. On increasing the argon flow rate, the scattering of boron atoms by argon is increased, resulting in rapid energy transfer and efficient thermalization. In contrast, lanthanum atoms are not affected as much by the scattering, because of their high atomic mass with respect to argon [28]. The increasing stoichiometry of the coatings at higher argon pressures is interpreted qualitatively by these scattering differences and is in good agreement with other investigations [28,29].

Increasing the bias voltage caused a gradual shift in the chemical composition of the coatings from B/La = 6.3 (grounded substrates) to B/La = 6.7 (bias voltage, −200 V). Taking into account the considerations discussed above, this behaviour may be explained by the implantation of the small boron atoms into the growing film by argon ions increasing with increasing bias voltage. This results in the formation of a lanthanum-enriched film surface, where the lanthanum atoms are preferentially resputtered with an increased bias voltage [30].

On increasing the substrate temperature in the range 150—250 °C, the B/La atomic ratio changes from 6.2 to 7.0, most probably because of differences in the temperature dependence of the sticking coefficients of the condensing atoms.

A typical XRD trace of a coating deposited onto a molybdenum substrate is shown in Fig. 4, where the relative peak heights of randomly oriented LaB_6 and molybdenum are indicated. In all cases, the formation of the LaB_6 phase could be unambiguously detected. As can be estimated from Fig. 4, the LaB_6 phase exhibits a strong (100) texture. The texture coefficients $TC_{(hkl)_j}$ are given by [31,32]

$$TC_{(hkl)_j} = \frac{(I_{(hkl)_j}/I_{(hkl)_{j,0}})}{(1/n)\sum_{i=1}^{n}(I_{(hkl)_i}/I_{(hkl)_{i,0}})} \quad (2)$$

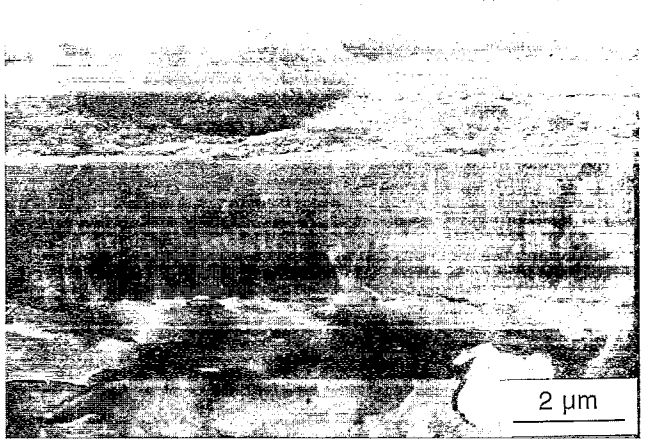

Fig. 2. Cross-sectional SEM image of a coating deposited onto a molybdenum substrate: sputtering power, 500 W; argon flow rate, 120 sccm; bias voltage, −100 V; substrate temperature, 200 °C.

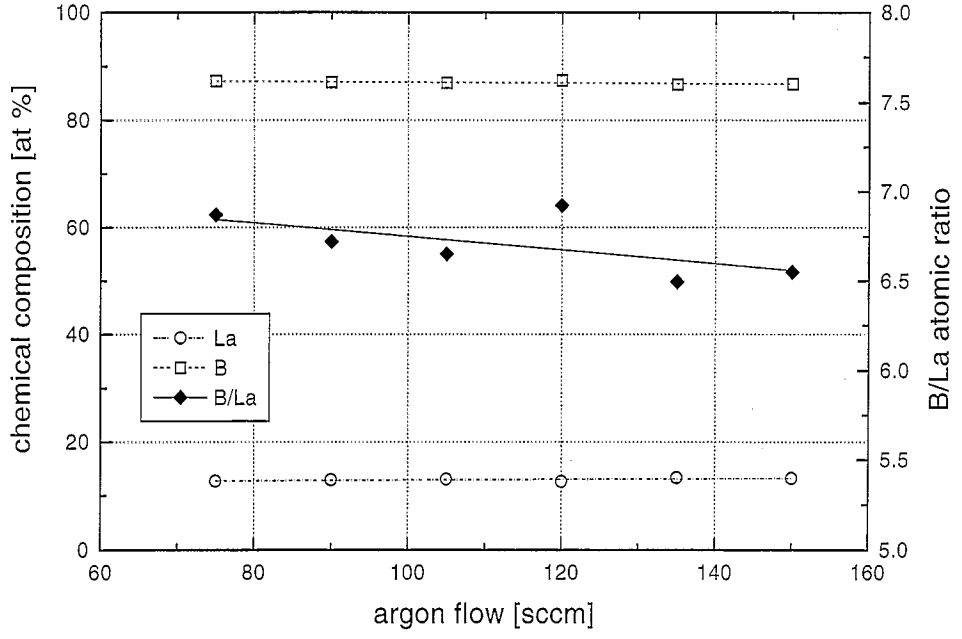

Fig. 3. Dependence of the chemical composition of the coatings on the argon flow rate: sputtering power, 500 W; bias voltage, −100 V; substrate temperature, 200 °C.

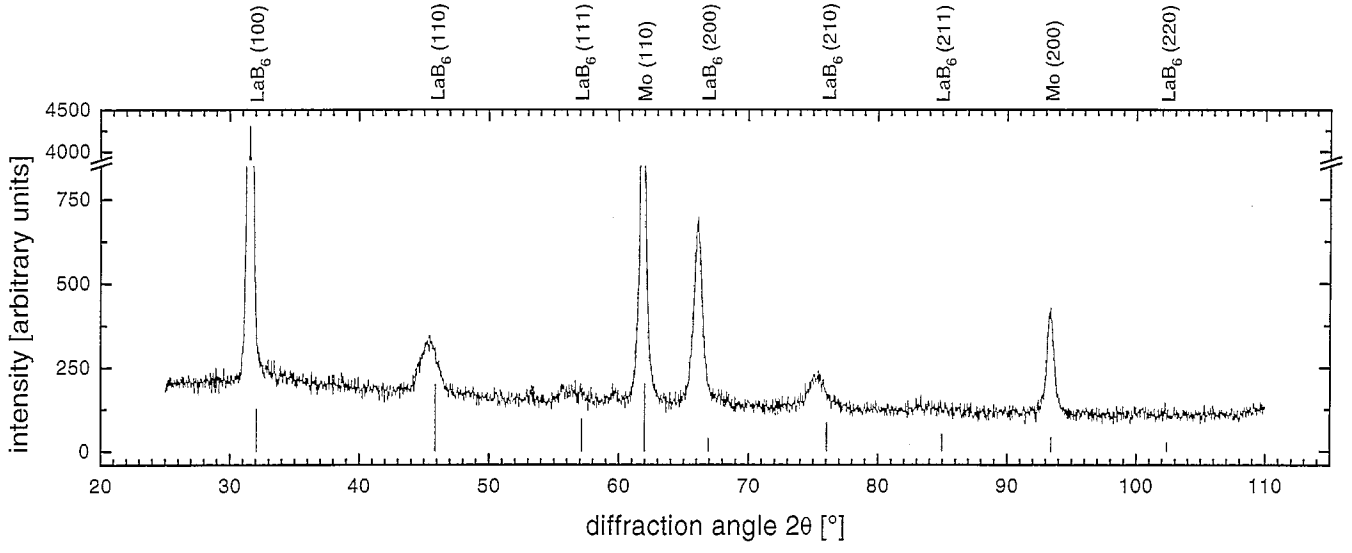

Fig. 4. Typical XRD trace of a coating deposited onto a molybdenum substrate: sputtering power, 500 W; argon flow, 105 sccm; bias voltage, −100 V; substrate temperature, 200 °C.

where I and I_0 are the intensity values for an (hkl) peak of interest taken from the XRD trace and the powder diffraction file, respectively, and n is the number of peaks considered.

The $TC_{(hkl)}$ values shown in Fig. 5(a) were calculated from the (100) and (110) peaks. The intensity values given in the JCPDS card [33] for Cu Kα radiation were corrected for the Cr Kα source used in this work, using the Lorentz polarization factor [34]. Because they were not present in all the spectra investigated or represent merely the second order of reflection, the (111), (210) and (200) peaks were not taken into account for the texture estimation given in Fig. 5(a). It should be noted that a random orientation would lead to TC values of unity, whereas a complete dominance of one peak would give a value of 2, i.e. the number n of peaks considered.

As can be seen clearly from Fig. 5(a), the distinct (100) orientation of the LaB_6 phase already inferred from Fig. 4 becomes even more dominant with increasing argon flow rate. At the same time, the lattice parameters derived from the diffraction peaks indicated in Fig. 5(b) show a lattice distortion relative to the standard value [33] (arrowed in Fig. 5(b)); this distortion is most marked in the (110) plane, falling asymptotically to the literature value as the argon flow rate is increased. While the full width at half-maximum (FWHM) values of the (100) and (200) peaks are nearly unaffected by the argon flow (0.3° and 0.6° respectively), we observed a strong

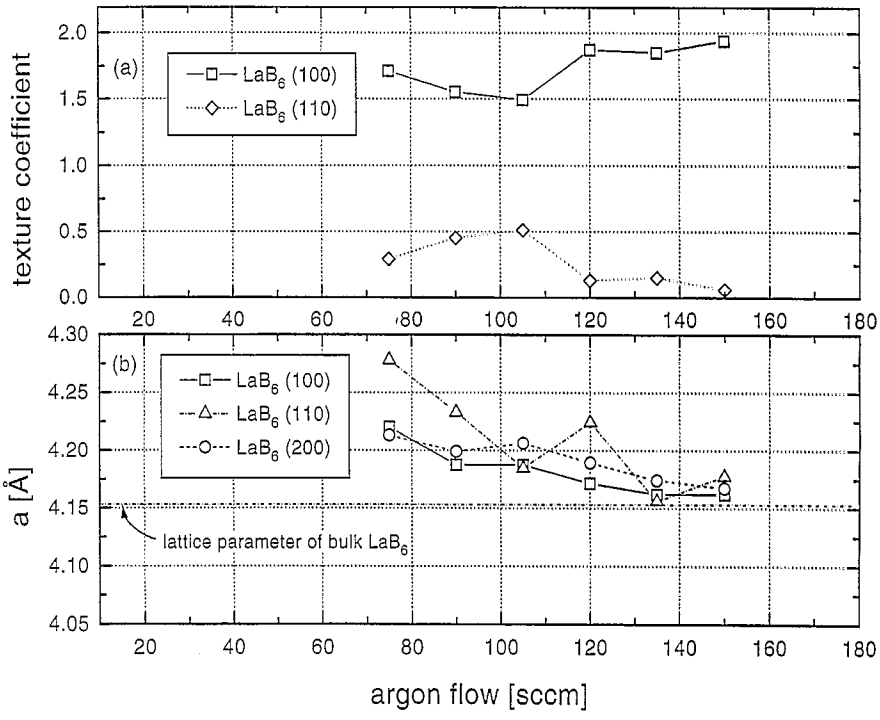

Fig. 5. (a) Texture coefficients and (b) lattice parameters obtained from XRD traces of coated molybdenum substrates as a function of the argon flow rate: sputtering power, 500 W; bias voltage, −100 V; substrate temperature, 200 °C.

decrease in the values for the (110) peak from 2.25° (argon flow, 75 sccm) to 0.65° (argon flow, 150 sccm). Obviously, the most preferred growth direction of the LaB_6 phase at high argon flow rates, i.e. condensation, nucleation, coalescence and crystal growth [35] by highly thermalized particles, is with the (100) planes parallel to the substrate surface, resulting in the formation of rather perfect crystals. The lattice distortions at low argon pressures (see Fig. 5(b)) are assigned to the effect of excess boron (cf. Fig. 3) and implanted argon atoms [36] incorporated interstitially into the LaB_6 lattice. Therefore, and as a result of the growth under distinct non-equilibrium conditions without complete coalescence [35], a slight misorientation of the (100) planes of the LaB_6 phase occurs (cf. Fig. 5(a)).

These results are in good agreement with those of Kinbara et al. [28] and Nakano et al. [37], who observed a shift in the preferred orientation from (100) to (111) through (110), by decreasing the argon pressure in the range between 5.0 and 0.2 Pa. They attributed this tendency to the different contributions of the strain and surface energy of the film. Within the range investigated, no pronounced effect of the deposition parameters of bias voltage (0 to −200 V) and substrate temperature (150–250 °C) on the XRD results was observed.

In Fig. 6 the variation of the Vickers microhardness values ($HV_{0.01}$) of the coatings deposited onto quenched and tempered steel substrates with the argon flow rate is shown. On increasing the process pressure, a distinct decrease in the film hardness from approximately 2900 $HV_{0.01}$ (argon flow, 75 sccm) to 1050 $HV_{0.01}$ (argon flow, 150 sccm) was observed. At first sight, a good correlation of the microhardness with the distortion of the LaB_6 lattice (cf. Fig. 5(b)) is achieved and the hardness values obtained at low flow rates are in good agreement with the literature values for bulk LaB_6 (in the range between 2600 HV_{50} [10] and 2150 $HV_{0.1}$ [15]). However, surprisingly low hardness values well below the literature values are observed for those coatings deposited at high argon pressures, although the B/La atomic ratio is close to stoichiometry (see Fig. 3) and the structure is less distorted (see Fig. 5(b)). In general, low particle energies and low substrate temperatures favour the formation of low strength grain boundaries, because of incomplete coalescence between growing crystals [35]. Therefore, in extremely fine-grained to fracture-amorphous structures, the well-known Hall–Petch relationship valid for comparatively large grain sizes may be overlapped by the high density of grain boundaries and voids [36]. In addition, internal stresses can be relaxed at open-voided grain boundaries. Thus, the low hardness values obtained at high argon flow rates are attributed to the extremely fine-grained to fracture-amorphous structure with low strength grain boundaries observed in these films.

On increasing the bias voltage, only a small increase in the film hardness from approximately 2100 (grounded substrates) to 2300 $HV_{0.01}$ (bias voltage, −200 V) could be determined. Within the range investigated, we observed no significant effect of the substrate temperature on the hardness values.

The results of colourimetric measurements based on

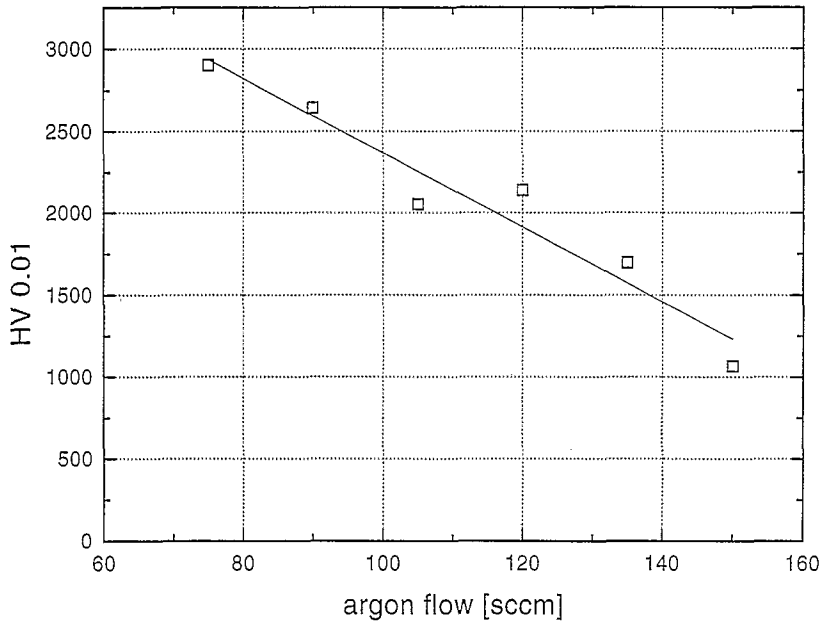

Fig. 6. Vickers microhardness values $HV_{0.01}$ of coatings deposited onto quenched and tempered steel substrates as a function of the argon flow rate: sputtering power, 500 W; bias voltage, −100 V; substrate temperature, 200 °C.

the CIE-$L^*a^*b^*$ method are presented in Fig. 7 as a function of the argon flow rate. With chromatic values a^* and b^* of approximately 7 and −10, respectively, the colouration of the coatings corresponds—fairly independently of the argon flow—to a violet hue. However, because of the marked decrease in the brilliance value L^* with increasing argon pressure, a change in the colouration with respect to human colour perception was observed, from violet (argon flow rate, $\leqslant$ 105 sccm) to almost black (argon flow rate, $\geqslant$ 135 sccm). In general, the visual impression of bulk LaB_6 with a more distinct red colour component was not obtained for the coatings deposited.

Considering the results obtained, there is a good agreement with the work of McKelvy et al. [12], who distinguished the purple stoichiometric LaB_6 from a blue-coloured randomly lanthanum-deficient hexaboride with composition $LaB_{6.13\pm0.03}$. However, it should be noted that structural defects, such as interstitials, vacancies and impurities, which are typical for coatings grown by low temperature physical vapour deposition processes, are expected to reduce the mobility and the

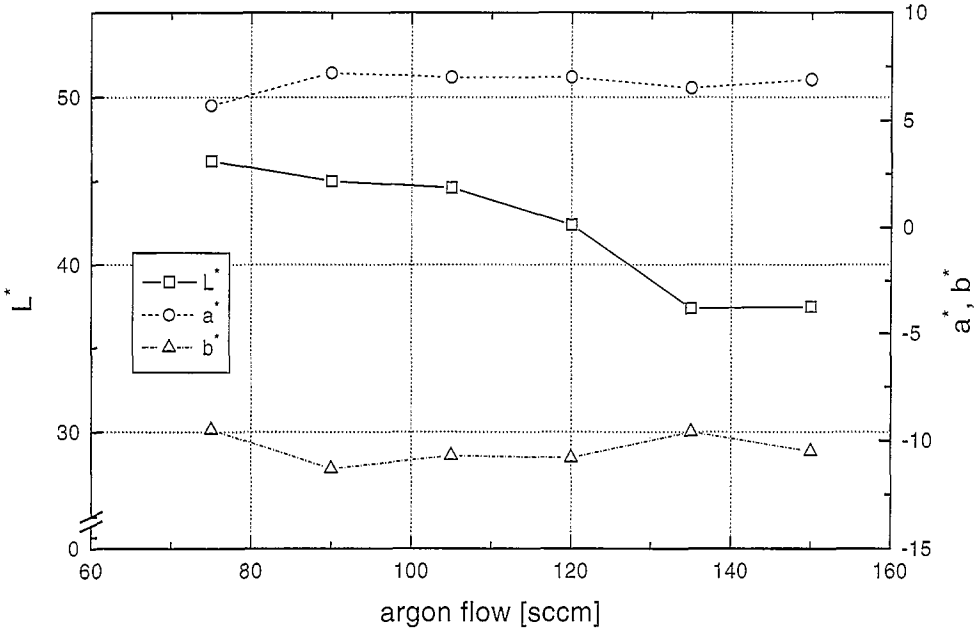

Fig. 7. Variations of CIE-$L^*a^*b^*$ colourimetric indexes of coatings deposited onto austenitic steel substrates with the argon flow rate: sputtering power, 500 W; bias voltage, −100 V; substrate temperature, 200 °C.

relaxation time of free electrons, so affecting the shape of the plasma oscillation edge [38]. Similar results on LaB_6-based coatings have been published by other groups [39,40]. The marked decrease in the brilliance value L^* with increasing argon flow rate must be attributed to the observed stoichiometric and structural changes. Obviously, the described tendency to form surface defects at low argon flow rates, which should lower the brilliance, is superposed by these mechanisms.

On increasing the bias voltage, we observed a slight shift of the a^* and b^* values from 8 and −12 (grounded substrates) to 6 and −10 (bias voltage, −200 V), respectively, whereas the brilliance value was nearly unaffected. Within the range investigated, the substrate temperature showed no pronounced effect on the colouration.

The main results of the analyses using EPMA, XRD, Vickers microhardness measurements and CIE-$L^*a^*b^*$ colour characterization are correlated in Fig. 8. With respect to the literature value of LaB_6 [33] (represented in Fig. 8 by a full square), all the films deposited show a distinct enlargement of the lattice parameter. Surprisingly, the correlation between the B/La atomic ratio and the lattice parameter of the LaB_6 phase is quite poor. We attribute this behaviour, in part, to the different deposition parameters summarized in Fig. 8 (although the correlation for the variation of the argon flow rate, for example, using constant values for the bias voltage and substrate temperature is also not pronounced) and to the effects that arise from the variation of these deposition parameters, such as the incorporation of argon atoms, or variations of the dislocation density or grain size [36], which have not been investigated within this study.

Despite these facts, we observed a good correlation between the hardness and the colouration (represented by the brilliance L^*, since the chromatic values are not affected very much (cf. Fig. 7)) of the coatings and the lattice parameter. The increase in the Vickers microhardness $HV_{0.01}$ to values well beyond those in the literature with increasing lattice distortion is attributed to the formation of close-packed grains and to the increased Peierls stress resulting in hindered dislocation mobility. Except for one film with a high density of surface defects that caused low brilliance, a linear increase in the L^* value with increasing distortion of the lattice was observed. A possible interpretation for this dependence may be given by the less marked absorption edges of materials with a high degree of structural disorder [38].

The results of the corrosion tests of the coated austenitic steel substrates in the saturated vapour of an artificial perspiration solution at 40 °C can be summarized as follows. Although the coatings themselves withstood the corrosion attack, in the case of those films deposited at low argon flow rates or high bias voltages, the perspiration solution penetrated into previously existing defects and microfissures, so gradually detaching the films. Films deposited under moderately energetic conditions, i.e. at high argon flow rates and low bias voltages or substrate temperatures, remained stable over the full test period of 288 h.

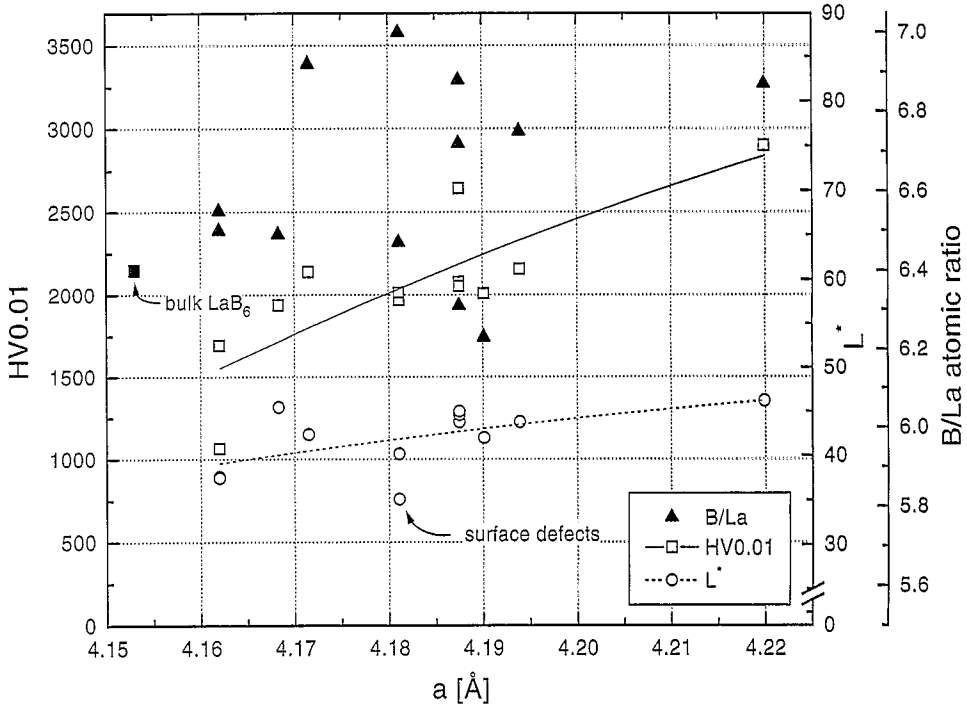

Fig. 8. Correlation between chemical composition, Vickers microhardness $HV_{0.01}$, brilliance value L^* and lattice parameter a (measured parallel to the (100) plane) of the LaB_6 phase: sputtering power, 500 W. (The full square indicates the literature values for the Vickers hardness and lattice parameter of bulk LaB_6 [15,33].)

4. Conclusions

Single-phase LaB_6, overstoichiometric coatings with fine-columnar to extremely fine-grained structures have been obtained by d.c. magnetron sputter deposition, using an LaB_6 target. The interrelationships between the chemical composition, crystal structure, hardness and colourations of these coatings could be established. With respect to the chemical composition, crystallinity and adhesion, the most favourable deposition conditions are high argon pressures and moderate bias voltages and substrate temperatures. However, the highest hardness values and the most marked visual colour impression are obtained at low gas pressures. With careful optimization of the films with respect to these points, their application as decorative violet coatings seems to be promising.

Acknowledgements

The authors are grateful to G. Hawranek (Institut für Metallkunde und Werkstoffprüfung, Montanuniversität Leoben) for his help in SEM characterization of the coatings and to Dr. B. Ortner (Institut für Metallphysik, Montanuniversität Leoben) for helpful discussions on the evaluation of the XRD traces. We would also like to thank Dr. P. Rödhammer (Metallwerk Plansee, Reutte) for supplying the molybdenum sheets and Dr. H. Baumann (Institut für Kernphysik, Universität Frankfurt) for RBS and ERD analysis.

References

[1] W. Schintlmeister and O. Pacher, *J. Vac. Sci. Technol., 4* (1975) 743.
[2] R.W. Johnson and A.H. Daane, *J. Phys. Chem., 65* (1961) 909.
[3] T. Niemyski and E. Kierzek-Pecold, *J. Cryst. Growth, 3–4* (1968) 162.
[4] G.V. Samsonov, Yu B. Paderno and V.S. Fomenko, *Poroshkovaya Metall., 6* (1963) 24 (in Russian).
[5] H.A. Jehn, in W. Gissler and H.A. Jehn (eds.), *Advanced Techniques for Surface Engineering*, Kluwer, Dordrecht, 1992, p. 359.
[6] B. Zega, *Surf. Coat. Technol., 39–40* (1989) 507.
[7] U. Kopacz and R. Riedl, *Z. Metallkd.*, 7 (1992) 492.
[8] B. Post, in K.S. Vorres (ed.), *Proc. 3rd Int. Conf. on Rare Earth Research*, Gordon and Breach, New York, 1963, p. 107.
[9] J. Etourneau, J.-P. Mercurio and P. Hagenmuller, in V.I. Matkovich (ed.), *Boron and Refractory Borides*, Springer, Berlin, 1977, p. 115.
[10] F. Binder, *Radex-Rundschau, 1* (1977) 52.
[11] P.A.M. van der Heide, H.W. ten Cate, L.M. ten Dam, R.A. de Groot and A.R. de Vroomen, *J. Phys. F, 16* (1986) 1617.
[12] M.J. McKelvy, L. Eyring and E.K. Storms, *J. Phys. Chem., 88* (1984) 1785.
[13] J. Stallmaier, C. Mitterer and J. Barounig, *Proc. 11th Int. Conf. on Vacuum Metallurgy, Le Vide, les Couches Minces, 261* (1992) 265.
[14] E. Brandstetter, C. Mitterer and R. Ebner, *Thin Solid Films, 201* (1991) 123.
[15] F. Binder, *Radex-Rundschau, 4* (1975) 531.
[16] B. McDonald and A. Goetzberger, *J. Electrochem. Soc., 109* (1962) 141.
[17] G.F. Bastien and H.J.M. Heijligers, *J. Microsc. Spectrosc. Electron., 11* (1986) 215.
[18] D. Hofmann, in H. Fischmeister and H. Jehn (eds.), *Hartstoffschichten zur Verschleißminderung*, DGM Informationsgesellschaft, Oberursel, 1987, p. 113.
[19] R.S. Uppadhye and E.J. Hsieh, *J. Vac. Sci. Technol. A, 8*(3) (1990) 1348.
[20] R. Elsing, *Surf. Coat. Technol., 49* (1991) 132.
[21] G.M. Turner, I.S. Falconer, B.W. James and D.R. McKenzie, *J. Vac. Sci. Technol. A, 10*(3) (1992) 455.
[22] G. Håkansson, J.-E. Sundgren, D. McIntyre, J.E. Greene and W.-D. Münz, *Thin Solid Films, 153* (1987) 55.
[23] I. Petrov, L. Hultman, U. Helmersson, J.-E. Sundgren and J.E. Greene, *Thin Solid Films, 169* (1989) 299.
[24] P.C. Johnson, in J.L. Vossen and W. Kern (eds.), *Thin Film Processes II*, Academic Press, San Diego, CA, 1991, pp. 242–244.
[25] G. Betz, M. Opitz and P. Braun, *Nucl. Instrum. Methods, 182–183* (1981) 63.
[26] J.A. Thornton, in R.F. Bunshah (ed.), *Deposition Technologies for Films and Coatings*, Noyes, Park Ridge, NJ, 1982, p. 181.
[27] M. Konuma, *Film Deposition by Plasma Techniques*, Springer, Berlin, 1992, p. 14.
[28] A. Kinbara, T. Nakano, A. Kobayashi, S. Baba and T. Kajiwara, *Appl. Surf. Sci., 70–71* (1993) 742.
[29] T. Kajiwara, T. Urakabe, K. Sano, K. Fukuyama, K. Watanabe, S. Baba, T. Nakano and A. Kinbara, *Vacuum, 41* (4–6) (1991) 1224.
[30] P. Losbichler, C. Mitterer, W.S.M. Werner, H. Störi and J. Barounig, *Thin Solid Films, 228* (1993) 56.
[31] A.J. Perry, *Thin Solid Films, 135* (1986) 73.
[32] A.J. Perry and J. Schoenes, *Vacuum, 36*(1–3) (1986) 149.
[33] Powder Diffraction File, Card 6-0401, Joint Committee on Powder Diffraction Standards, Swarthmore, PA, 1950.
[34] B.D. Cullity, *Elements of X-ray Diffraction*, Addison-Wesley, Reading, MA, 1978, p. 131.
[35] P.B. Barna, in L. Eckertová and T. Růžička (eds.), *Diagnostics and Applications of Thin Films*, Institute of Physics, Bristol, 1992, p. 295.
[36] J.-E. Sundgren, *Thin Solid Films, 128* (1985) 21.
[37] T. Nakano, S. Baba, A. Kobayashi, A. Kinbara, T. Kajiwara and K. Watanabe, *J. Vac. Sci. Technol. A, 9*(3) (1991) 547.
[38] R.E. Hummel, *Electronic Properties of Materials*, Springer, Berlin, 1993.
[39] S. Winsztal, H. Majewska-Minor, M. Wiśniewska and T. Niemyski, *Mater. Res. Bull., 8* (1973) 1329.
[40] K.R. Peschmann, J.T. Calow and K.G. Knauff, *J. Appl. Phys., 44*(5) (1973) 2252.